



Effects of illite–smectite clay minerals on the thermal evolution of aliphatic organic matter–clay complexes: a study with thermogravimetry coupled with Fourier transform infrared spectroscopy (TG-FTIR)

Hongling Bu^{1,2} · Yanfu Wei³ · Chengshuai Liu¹ · Dong Liu² · Daoyong Tan⁴ · Hongmei Liu²

Received: 6 February 2022 / Accepted: 21 November 2022 / Published online: 7 December 2022
© Akadémiai Kiadó, Budapest, Hungary 2022

Abstract

Illite–smectite (I–Sm) clay minerals widely existed in clay-rich rocks or sediments. Understanding the effects of I–Sm clay minerals on the thermal evolution of organic matters (OMs) may facilitate interpreting hydrocarbon generation levels in petroleum basins and the global organic carbon cycle. In this study, mixed-layer I–Sm mineral rectorite (Rec), end-members montmorillonite (Mnt), and illite (Ilt) were chosen as the typical clay minerals and aliphatic organic compounds with different functional groups were selected as model OMs. Two kinds of OM–clay complexes, including OM–clay mixtures and OM–clay interlayer composite, were prepared. Pyrolysis experiment of OM–clay complexes were conducted via thermogravimetry coupled with Fourier transform infrared spectroscopy (TG-FTIR). TG-FTIR analysis showed that I–Sm clay minerals influenced the main thermal decomposition temperature (T_M) and gas products of pyrolyzed OMs. Both Rec and Mnt decreased the T_M of OMs and promoted decarboxylation, and the effect of Rec on T_M was more obvious. Ilt had no significant effect on the T_M and decarboxylation. Physicochemical property of the minerals showed that the solid acidity of the clay mineral was the key factor for the T_M and types of thermal decomposition reaction (i.e., decarboxylation and C–C cleavage). Further analysis indicated that the functional groups of OMs affected the pyrolytic behaviors of OMs. OMs with cationic groups can be intercalated into the interlayers of clay minerals, which thus exhibited a high thermal stability. Functional groups such as alkyl chain and carboxyl groups had different binding effect with clay minerals, which leading to a difference of T_M . Our results provide new insights into the role of I–Sm clay minerals in hydrocarbon generation in fine-grained sedimentary rocks as well as the geochemical behavior of organic carbon in response to inorganic minerals.

Keywords Mixed-layer illite/smectite mineral · Solid acidity · Thermal degradation · Fatty acid · Hydrocarbon generation

Hongling Bu and Yanfu Wei have contributed equally to this work.

✉ Hongling Bu
hlbu@soil.gd.cn; buhongling@gdut.edu.cn

¹ Guangdong Key Laboratory of Integrated Agro-Environmental Pollution Control and Management, Institute of Eco-Environmental and Soil Sciences, National-Regional Joint Engineering Research Center for Soil Pollution Control and Remediation in South China, Guangdong Academy of Sciences, Guangzhou 510650, China

² CAS Key Laboratory of Mineralogy and Metallogeny/Guangdong Provincial Key Laboratory of Mineral Physics and Materials, Guangzhou Institute of Geochemistry, Institutions of Earth Science, Chinese Academy of Sciences, Guangzhou 510640, China

³ National Observation and Research Station of Coastal Ecological Environments in Macao, Macao Environmental Research Institute, Macau University of Science and Technology, Taipa, Macao 999078, China

⁴ Key Laboratory of Solid Waste Treatment and Resource Recycle, Sichuan Engineering, Lab of Non-Metallic Mineral Powder Modification & High-Value Utilization, Ministry of Education, Southwest University of Science and Technology, Mianyang 621010, China

Introduction

Most of the petroleum hydrocarbon was generated and occurred in fine-grained sedimentary rocks (i.e., shales). Clay minerals are the predominant components in these rocks, especially for gas-bearing shales. These clay minerals include montmorillonite, illite, mixed-layer illite–smectite (I–Sm) minerals. Montmorillonite is a 2:1 expanding clay mineral that has two Si–O tetrahedral sheets sandwiching a central Al–O octahedral sheet. Considerable substitution occurred in the octahedral sheet (i.e., substitution of Mg^{2+} for Al^{3+}) and tetrahedral sheets (substitution of Al^{3+} for Si^{4+}). Due to isomorphous substitution in the octahedral sheet, some exchangeable hydrated ions may appear in the interlayer space of montmorillonite, i.e., Ca^{2+} , Na^+ [1]. Illite is a non-expanding 2:1 clay mineral, and the interlayer space of illite is mainly occupied by poorly hydrated K^+ . Mixed-layer I–Sm clay mineral is the intermediate composition between end-members of montmorillonite and illite. In different sedimentary environment, the assemblage pattern of these I–Sm clay minerals groups varies significantly [2].

I–Sm clay minerals had valuable geological participators in petroleum basin and played an important role in organic matters (OMs) accumulation [3] and petroleum hydrocarbon generation [4, 5], which thus have been focused by many researchers. For instance, I–Sm clay minerals were found to be closely related to the hydrocarbon accumulation in some sedimentary basins [6–8]. Especially, the occurrence of mixed-layer I–Sm minerals was related to petroleum accumulation [9]. In addition, there was a coincidence between the temperatures for the I–Sm minerals conversion from the random to ordered interstratified and those for the onset of oil generation peak in some sedimentary, showing that changes in the ordering of mixed-layer I–Sm minerals were particularly important in the exploration for hydrocarbons occurrence [10].

Considering this phenomenon, the thermal evolution or degradation of OMs with I–Sm clay minerals in experimental system has been studied during the last two decades. The experiments on heating petroleum source rocks or OMs (i.e., kerogen, fatty acids, and other organic compounds) are often used to simulate hydrocarbon generation processes and identify the organic–inorganic interactions within the formation of petroleum in nature [11, 12]. These studies indicated that I–Sm clay minerals have an influence on hydrocarbon generation by cracking of OM, controlling the pyrolysis maturity indicator, pyrolysis reaction (i.e., isomerization) gas-to-oil ratio, gas wetness, and fluid aromaticity pyrolysate [13–18]. The inherent solid acidity (the proton-donating capability or ability of being an electron pair acceptor) of clay minerals has been linked with the development of complex organic networks (i.e., kerogen) and cracking of kerogen or bitumen

phase to produce hydrocarbons [19–22]. Thus, understanding the effect of I–Sm clay minerals on thermal evolution of OMs is essential for comprehending the processes and mechanisms of the evolution of OMs-involved clay minerals in the petroleum basins.

Previous work studied the effect of clay minerals on hydrocarbon generation or thermal degradation of OMs through various pyrolysis experiments in the open or closed laboratory heating system. In most pyrolysis experiments, the possibility that organics react with surface of minerals (including outer- and inner-surfaces) was not considered. In fact, OMs could be usually associated with clay minerals through several processes, such as adsorption, bounding, and intercalation [5, 8, 11, 17]. The multiple organic components (i.e., kerogen) were selected for these experiments, making it difficult to investigate the effect of surface properties (i.e., solid acidity) and microstructure of minerals on the hydrocarbon generation of pyrolyzed OM, and interface interaction of inorganic–organic became elusive. Even though some studies have considered the association between clay minerals and OMs and investigated the evolution of OM–clay associations with respect to thermal maturity in organic-rich source rocks [23]. Nevertheless, clay mineral assemblage (i.e., rocks) was commonly considered for these pyrolysis experiments. However, the clay mineral assemblage of natural samples possesses complex structure and mineral phase. Moreover, the coexistence of randomly and ordered interstratified mixed-layer I–Sm minerals made the analysis of the organic–inorganic interactions more difficult. The mixed-layer I–Sm mineral is a coherent stack of 2:1 layer having both illite and smectitic sheets [24]. As the mixed-layer I–Sm mineral became illitic, the interlayer arrangements gradually evolved from random to short-range ordered, and finally to long-range ordered [25]. According to ratios of smectite layer, the mixed-layer I–Sm minerals can be divided into two types: such as mixed-layer random I–Sm ($R=0$; amounts of illite layer is less than 50%) and mixed-layer ordered I–Sm (amounts of illite layer is more than 50%). Hence, the microstructure is different from each other and differs from montmorillonite and illite. Therefore, it is necessary for us to use one kind of clay mineral alone to prepare the pyrolysis experiment.

In this work, we investigated the contribution of I–Sm clay minerals to thermal decomposition of OMs using an atmospheric pyrolysis experiment. We hypothesized that these clay minerals play an unaccounted role in gaseous hydrocarbon, where mixed-layer I–Sm mineral could enhance hydrocarbon formation. To test this hypothesis, we characterized the relationship between the microstructure and solid acidity of I–Sm clay minerals and the chemical and spectroscopic characteristics of thermal OMs. Thermogravimetry coupled with Fourier transform infrared spectroscopy (TG-FTIR) was applied for thermal degradation

assessment of the OMs. It can detect changes in the mass loss of samples during heating and can simultaneously integrate evolved gas information (i.e., the gaseous products). Some analysis methods such as X-ray diffraction (XRD), FTIR, and solid acidity analysis were used to characterize the I-Sm clay minerals.

Materials and methods

Materials

Some aliphatic organic compounds were selected as the model OMs, including fatty acids, fatty amine, and alkane, for that this organic compound were regarded as some important precursors of hydrocarbons [26, 27]. Octadecanoic acid (OA, $\text{CH}_3(\text{CH}_2)_{16}\text{COOH}$), octadecyl trimethyl ammonium bromide (OTAB, $\text{CH}_3(\text{CH}_2)_{16}\text{CH}_2\text{N}(\text{CH}_3)_3\text{Br}$), n-octadecane (ODE, $\text{CH}_3(\text{CH}_2)_{16}\text{CH}_3$) were chosen. These model organic material (with a purity of 95 mass%) were obtained from Aldrich, Milwaukee, WI, USA. These organic compounds were used based on the following considerations. First, they possess relatively simple structures, and thus it is easier to be analyzed than organic compounds with complex compositions and structures, such as kerogen. Second, this kind of OMs contains carboxyl groups, alkyl chains, and a carboxylate group attached to a long chain hydrocarbon, which are common in natural organics such as in low-rank coals [28–30]. Third, the decarboxylation and cracking of aliphatic OMs (i.e., fatty acid) are proposed to be closely related to petroleum generation [26, 31, 32]. Therefore, investigating its thermal evolution behavior is of great significance to the exploration of petroleum formation in clay-rich rocks.

Rectorite (Rec), the mixed-layer I-Sm minerals with 50% S%, was selected as the typical mixed-layer I-Sm minerals. It is regular interstratification of one layer of illite and one-layer smectite (...ISIS...) with the value of $R=1$. In some shale or coal samples, Rec is one of the important mineralogical assemblages [33, 34]. Because this kind of mineral commonly occurred in clay-rich rocks and this clay mineral composition in sedimentary basins was found to be closely related to hydrocarbon accumulation. Particularly, it was found that the illitization of smectite corresponded with the evolution of OM that began to enter the threshold of oil generation [10]. Hower et al. (1976) [6] even showed the R1-ordered mixed-layer I-Sm

minerals correlated with oil generation. The structural formula of Rec was $(\text{Na}_{0.45}\text{K}_{0.32}\text{Ca}_{0.37}\text{Mg}_{0.08})(\text{Al}_{3.78}\text{Fe}_{0.11}\text{Ti}_{0.10})[(\text{Si}_{6.22}\text{Al}_{1.78})\text{O}_{20}](\text{OH})_4\cdot n\text{H}_2\text{O}$ [35]. The purity of Rec used in this study was very high, and less than 5% quartz occurred in Rec. Montmorillonite (Mnt) (with purity of > 95%) was collected from Inner Mongolia, China. Illite (Ilt) was sourced from Jilin Province, China. Based on the results of chemical analysis, the structural formula of Mnt was: $\text{Ca}_{0.168}\text{Na}_{0.025}\text{K}_{0.013}[\text{Si}_{3.984}\text{Al}_{0.016}][\text{Al}_{1.352}\text{Fe}_{0.271}\text{Mg}_{0.365}\text{Ti}_{0.010}]\text{O}_{10}(\text{OH})_2\cdot n\text{H}_2\text{O}$. By purification and exchange of sodium, the product of Mnt was obtained. The structural formula of Ilt (with purity of > 95%) is as follows: $\text{K}_{0.571}\text{Ca}_{0.010}\text{Na}_{0.028}[(\text{Al}_{1.853}\text{Fe}_{0.083}\text{Mg}_{0.032}\text{Ti}_{0.023}\text{P}_{0.009})-(\text{Si}_{3.331}\text{Al}_{0.667})\text{O}_{10}](\text{OH})_2\cdot n\text{H}_2\text{O}$.

The OM-clay mixtures were prepared to make the mineral and OMs mix evenly. Clay mineral sample was mechanically mixed with organic compound at a ratio of 4:1 (mass ratio). The products were denoted as OM-clay, i.e., OA-Rec, OTAB-Rec, and ODE-Rec. For OTAB, an OM-clay composite was prepared according to previous studies through a cation exchange method [17]. The OM-clay composite was denoted OTAB-Rec_{com}. The basal reflection obtained from XRD patterns and TOC content of each sample determined by elemental analysis are listed in Table 1. Compared with clay minerals alone, there was no obvious change in these d_{001} values in the (001) reflections of OM-clay mixture. These data indicated that the OM was not intercalated into the interlayer space of clay minerals for the OM-clay mixtures, and the organics only existed outside of clay minerals. However, for ODE-Rec and OTAB-Rec_{com}, which showed d_{001} values of 2.54–3.13 nm, respectively. It implied that a small amount of ODE entered the interlayer space of Rec, and OTAB successfully intercalated into the interlayer space of Rec. The corresponding results are shown in Figure S1 and S2 in part I of Supplementary material (SM).

Analysis methods

An elemental analyzer (Elementar Vario EL III Universal CHNOS) was used for detecting the TOC content of samples. X-ray diffraction (XRD) pattern was used to analysis the microstructure of clay minerals, OM-clay mixtures, and OM-clay composite. Powdered XRD analysis was performed with a Ni filter and Cu $K\alpha$ radiation (40 kV and 40 mA) on a Bruker D8 Advance diffractometer. The patterns were collected from $1^\circ 2\theta$ to $40^\circ 2\theta$ at the scanning rate of $1^\circ(2\theta)\text{ min}^{-1}$. FTIR spectra were used to investigate the

Table 1 The d_{001} values and the total organic content (TOC) of I-Sm clay minerals and OM-clay complexes

Samples	Rec	Mnt	Ilt	OA-Rec	OA-Mnt	OA-Ilt	OTAB-Rec	OTAB-Rec _{com}	ODE-Rec
d_{001}/nm	2.41	1.26	1.00	2.43	1.26	1.00	2.45	3.13	2.54
TOC (mass% sample)	–	–	–	20	20	20	20	17.22	20

composition and structural properties of clay minerals, as well as the bond of the elements. Sample in pressed KBr pellets were recorded on a Bruker Vertex-70 FTIR spectrometer. The spectra were collected at a resolution of 4 cm^{-1} with 64 scans for each measurement. The corresponding results are shown in Figure S3 in part II of SM.

Clay mineral influencing hydrocarbon generation is because the inherent surface solid acidity, which can catalyze reactions by energy transfer processes, redox reaction, and stabilization of intermediates [36]. Two types of surface solid acidity center distinguished in clay minerals, i.e., Brønsted acidity (B) and Lewis acidity (L). B and L acid sites were often differentiated by using diffuse reflectance Fourier transform infrared spectroscopy (DRIFT) with pyridine as a probe molecule [37]. The amount of total solid acid sites (Q_T) of clay minerals was determined by n-butylamine titration with Hammett indicators according to Liu et al. [37]. The amount of B acid sites (Q_B) of clay minerals was obtained from the product of the peak area ratio and the Q_T . The amount of Lewis acid (Q_L) of clay minerals was obtained by subtracting Q_B from Q_T . Detailed steps can be found in previous references [37]. The corresponding results are shown in Figure S4 in part III of SM.

Pyrolysis experiment

The pyrolysis experiments of samples were studied by using an in situ TG (NETZSCH STA 449C, Germany) coupled with a Bruker Vertex-70 FTIR. Approximately 10 mg of OM-clay complexes were heated from room temperature to 900 °C at a rate of 20 °C min^{-1} in an argon flow (99.99% purity, $40\text{ cm}^3\text{ min}^{-1}$). Before testing, the instruments were temperature-corrected by the melting point of the standard metal. The spectrometer was connected to the TG analyzer through a polytetrafluoroethylene transfer line and a gas cell that were both heated to 200 °C . Three-dimensional (3D) spectrogram was obtained through real-time detection of the OMs pyrolysis process.

Results

The temperature at which maximum mass loss occurred was defined as the main thermal decomposition temperature (T_M) in this study. One DTG peak was observed at 305 °C for pure OA (Fig. 1b), indicating that the thermal evolution of OA occurred in the range of $200\text{--}350\text{ °C}$ (Fig. 1a) and the T_M of OA was 305 °C . The corresponding evolved gases at T_M showed strong bands at $2934\text{--}2864\text{ cm}^{-1}$ (Fig. 2a), which were related to the antisymmetrical and symmetrical stretching of CH_2 groups [38], respectively. These bands indicated that aliphatic hydrocarbon fragments were the major gaseous products at this stage. In addition, a band at 1108 cm^{-1}

appeared (Fig. 2a), which was related to C–O–C stretching vibration [39]. This occurrence of this band indicated the presence of some small amounts of carboxylic acid. Carboxylic acid was also identified at $3573\text{--}1779\text{ cm}^{-1}$ [39, 40]. These bands suggested that the mass loss process of OA might be a degradation not a simple evaporation/desorption, even though some small mass loss of pure OA was possibly attributed to the sublimation of OA. Pure OA was decomposed via cleavage of C–C bonds, which led to the production of aliphatic hydrocarbons and carboxylic acid.

For OA-Rec sample as shown in Fig. 1c, a DTG peak at 104 °C occurred below 200 °C owing to the release of the water from Rec (Figure S5 in part IV of SM). A sharp DTG peak was resolved at 276 °C in the DTG curve of OA-Rec (Fig. 1d). This result meant the T_M in OA-Rec was lower than that of OA decreased by approximately 29 °C . This indicated that the thermal degradation of OA was strongly promoted by Rec. A similar phenomenon occurred in the OA-Mnt sample, the T_M in OA-Mnt was 289 °C , which was 16 °C lower than the pure OA (Fig. 1d). Additionally, a smaller DTG peak was read at 435 °C , which may be due to some OM that was pyrolyzed spontaneously and was unaffected by clay minerals located in peripheral positions [41]. For the OA-Itt sample, only one DTG peak occurred at 302 °C (Fig. 1d), indicating that Itt had almost no effect on the T_M of OA. The T_M of OA in the OA-clay mixture was changed by the presence of clay minerals (Fig. 1c and d), and so was gaseous products such as CO_2 ($2323\text{--}2370\text{ cm}^{-1}$) and methyl gaseous hydrocarbons (Fig. 3). CO_2 and methyl gaseous hydrocarbons were only occurred in OA-Rec and OA-Mnt (Fig. 3a and b). The results suggested that both C–C bond breakage and decarboxylation reactions were primary thermal reactions during the pyrolysis of OA in the presence of Rec and Mnt. The relative areas ratios of the FTIR bands at 2361 and $\sim 1777\text{ cm}^{-1}$ at T_M was 0.000 for OA, 0.294 for OA-Rec, and 0.802 for OA-Mnt. These relative areas ratio referred to the ratios of CO_2 to carboxylic acid in their gaseous products, which implied that the decarboxylation of OA was significantly promoted by Mnt at T_M .

For OTAB, T_M in OTAB alone occurred at 272 °C (Fig. 1b), while it in OTAB-Rec and OTAB-Rec_{com} occurred at $241\text{--}428\text{ °C}$, respectively (Fig. 1f). It indicated that the Rec had significant effect on the T_M of OTAB. The small DTG peak of OTAB-Rec at 428 °C indicated that a small part of OTAB had intercalated into the interlayer space of Rec, which agreed with the XRD data (Figure S2). The DTG peaks at $269\text{--}342\text{ °C}$ in OTAB-Rec_{com} implied that the pyrolysis of OTAB was delayed by the interlayer space of Rec. Aliphatic hydrocarbons were the mainly gaseous products that evolved from OTAB (Fig. 2b). The bands of antisymmetrical and symmetrical stretching of CH_2 groups ($2933\text{--}2863\text{ cm}^{-1}$), CH-stretching (2823 and 2775 cm^{-1}), CH_3 -bending (1460 cm^{-1}), and CH_3 -rocking (1289 cm^{-1})

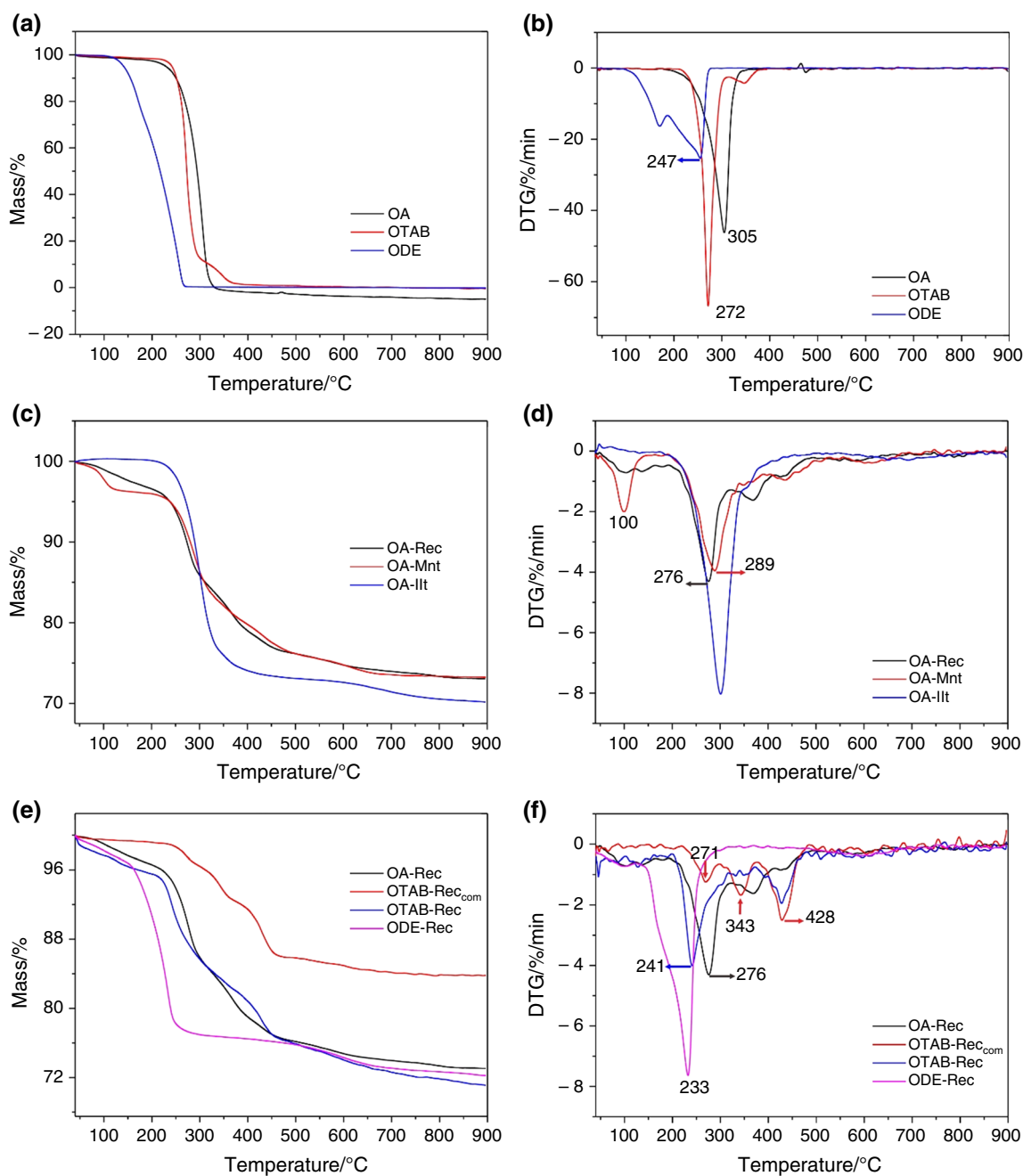


Fig. 1 TG-DTG curves of OMs and OM-clay complexes. **a** TG curves of OA, OTAB, and ODE; **b** DTG curves of OA, OTAB, and ODE; **c** TG curves of OA-Rec, OA-Mnt, and OA-Itt; **d** DTG curves

of OA-Rec, OA-Mnt, and OA-Itt; **e** TG curves of OA-Rec, OTAB-Rec, OTAB-Rec_{com}, and ODE-Rec; **f** DTG curves of OA-Rec, OTAB-Rec, OTAB-Rec_{com}, and ODE-Rec

confirmed the generation of aliphatic hydrocarbons. However, for OTAB-Rec, a CO₂ band (2361 cm⁻¹) was occurred (Fig. 4a), which was due to the pyrolysis of residual OM in Rec. In addition to this, a band was observed at 1701 cm⁻¹ (Fig. 4a, b), which was attributed to the C=C stretching vibration, indicating that there are alkenes in the products. However, the product of alkenes was almost only appeared in the case of OTAB-Rec_{com} at higher temperature

(342–428 °C) (Fig. 4b). These different products implied various reaction pathways existed during the pyrolysis of OTAB-Rec and OTAB-Rec_{com}.

For ODE, ODE decomposed completely 300 °C and one DTG peak observed at 247 °C (Fig. 1b). Aliphatic hydrocarbons were the main gaseous products, which showed characteristics bands at 2933, 2864, 1463 cm⁻¹ (Fig. 2c). The antisymmetric CH₃-stretching vibration (2967 cm⁻¹)

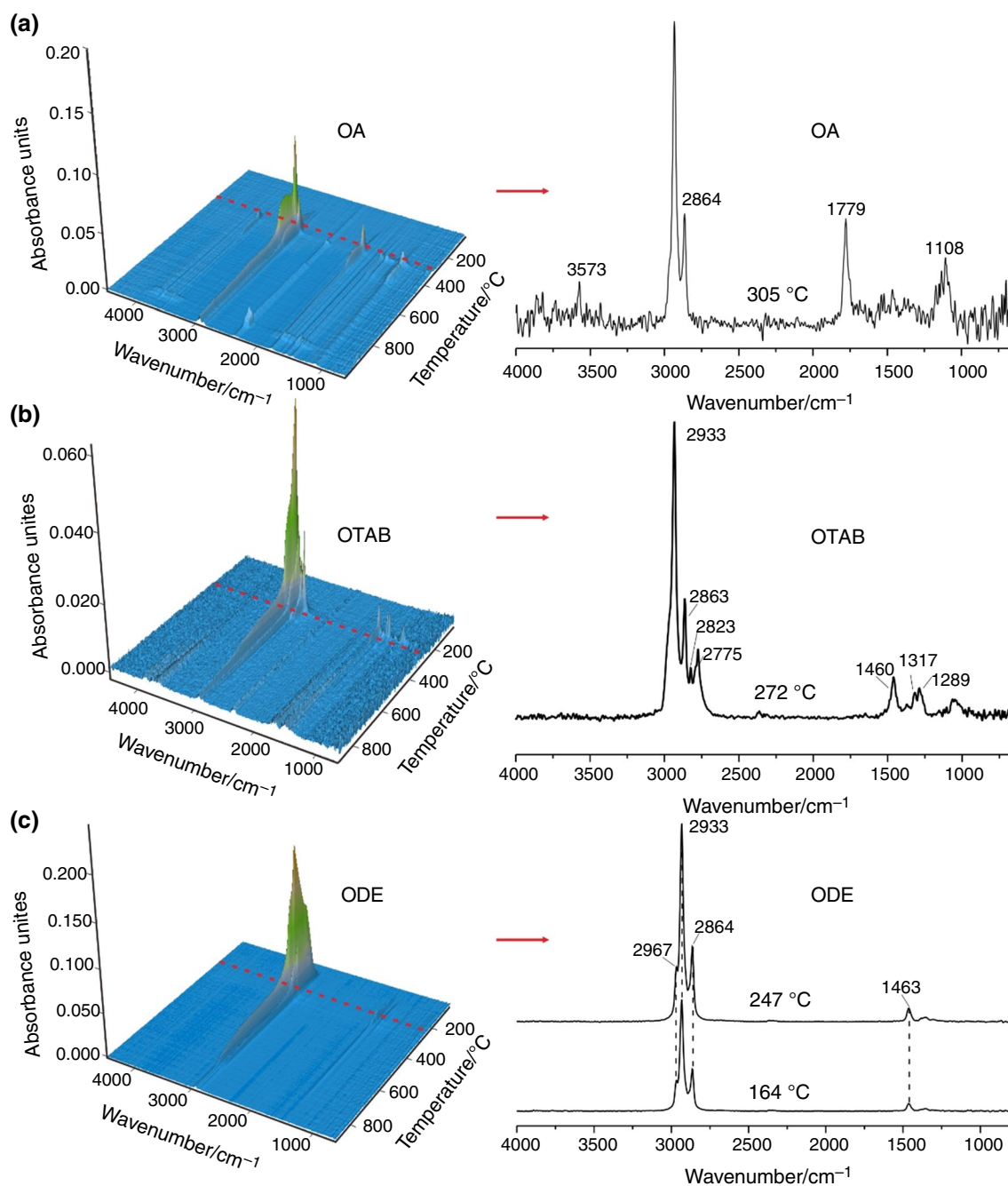


Fig. 2 3D-FTIR spectra of OMs and FTIR spectra of the evolved gases from pyrolyzed OMs at temperature of the maximum evolution rate. **a** 3D-FTIR spectra of OA; **b** FTIR spectra of the evolved gases from pyrolyzed OA at 305 °C; **c** 3D-FTIR spectra of OTAB; **d**

FTIR spectra of the evolved gases from pyrolyzed OTAB at 272 °C; **e** 3D-FTIR spectra of ODE; **b** FTIR spectra of the evolved gases from ODE at 164–247 °C

suggested the presence of methyl gaseous hydrocarbons. The T_M of 233 °C were found in the case ODE-Rec (Fig. 1f), and the types of the main gaseous products were almost the same with that of the ODE alone (Fig. 4c). The relative areas of the bands at 2933 cm^{-1} at T_M were evaluated to quantitatively compare the amounts of aliphatic hydrocarbons in the presence and absence of Rec. This relative area was

1.06/mg TOC for ODE and 2.54/mg TOC for ODE-Rec, which implied that Rec promoted the production of aliphatic hydrocarbons.

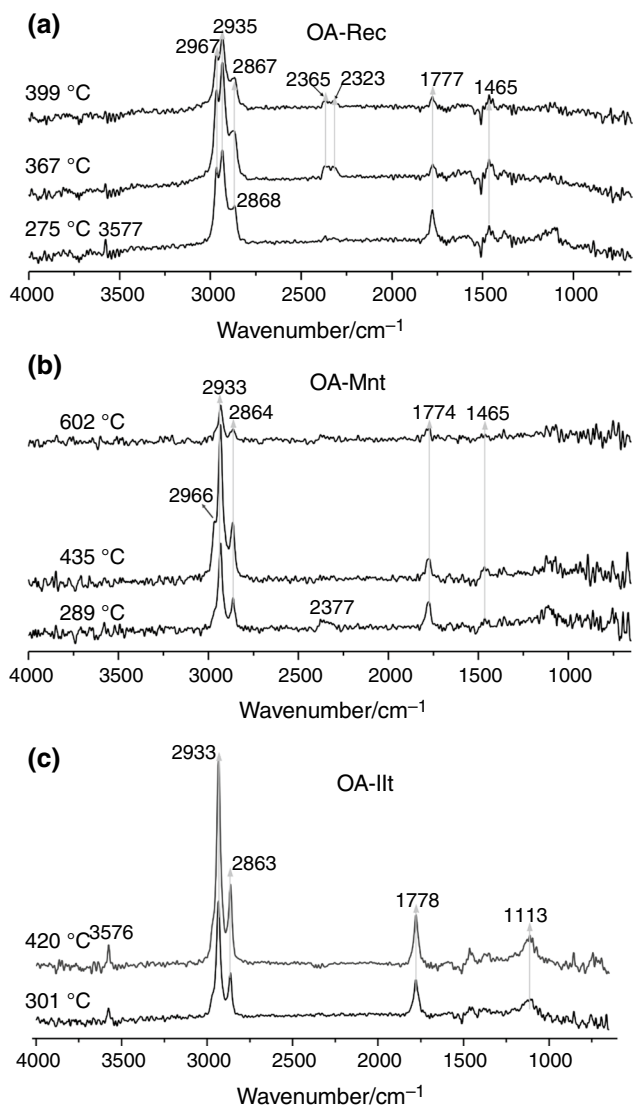


Fig. 3 FTIR spectra of the evolved gases from pyrolyzed OA-clay mixture samples at temperature of the maximum evolution rate. **a** FTIR spectra of the evolved gas from OA-Rec at 275 °C, 367 °C, and 399 °C; **b** FTIR spectra of the evolved gases from OA-Mnt at 289 °C, 435 °C, and 602 °C; **c** FTIR spectra of the evolved gases from OA-Ilit at 301–420 °C

Discussion

Effect of clay mineralogy on the thermal evolution of OM-clay complexes

Previous studies demonstrated that hydrocarbon generation of OMs were largely depended on the clay mineralogy of I-Sm minerals [10, 17]. In this study, three types of I-Sm clay minerals including Rec, Mnt, and Ilit were used to evaluate the effect of clay mineralogy on the thermal evolution of OMs. The effect of Rec for pyrolyzed OA was greater than that of Mnt on that of T_M . Ilit had no significant effect

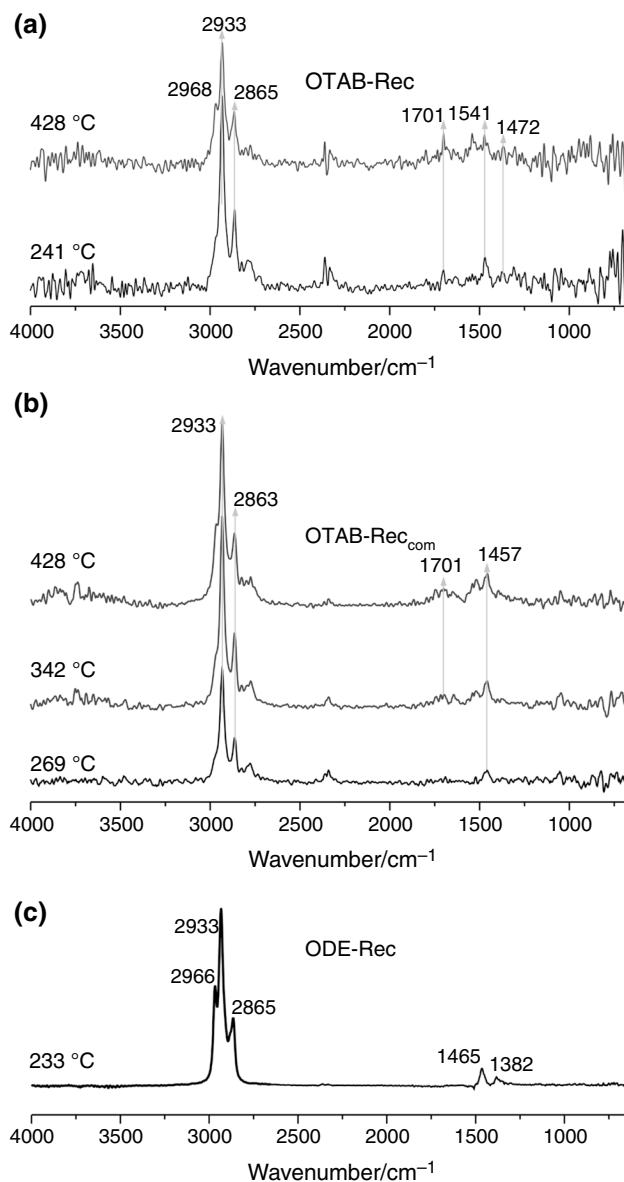


Fig. 4 FTIR spectra of the evolved gases from pyrolyzed OM-Rec complexes at temperature of the maximum evolution rate. **a** FTIR spectra of the evolved gases from OTAB-Rec at 241–428 °C; **b** FTIR spectra of the evolved gases from OTAB-Rec_{com} obtained at 269 °C, 342 °C, and 428 °C; **c** FTIR spectra of the evolved gases from ODE-Rec obtained at 233 °C

on the T_M and gas products (Figs. 1d and 3c). The identified gaseous species (hydrocarbons and CO₂) and temperature changes were analyzed (Fig. 5a and c). The result indicated that the hydrocarbons release peak temperature in OA-Mnt (440 °C) was higher than that of OA-Rec (294–376 °C), and the CO₂ release peak temperature in the case of OA-Mnt (308 °C) was lower than in the case of OA-Rec (353 °C). It suggests the C–C cleavage reaction and decarboxylation of OA generally depended on the clay mineralogy. Abundant B acid sites in Rec are important factors influencing

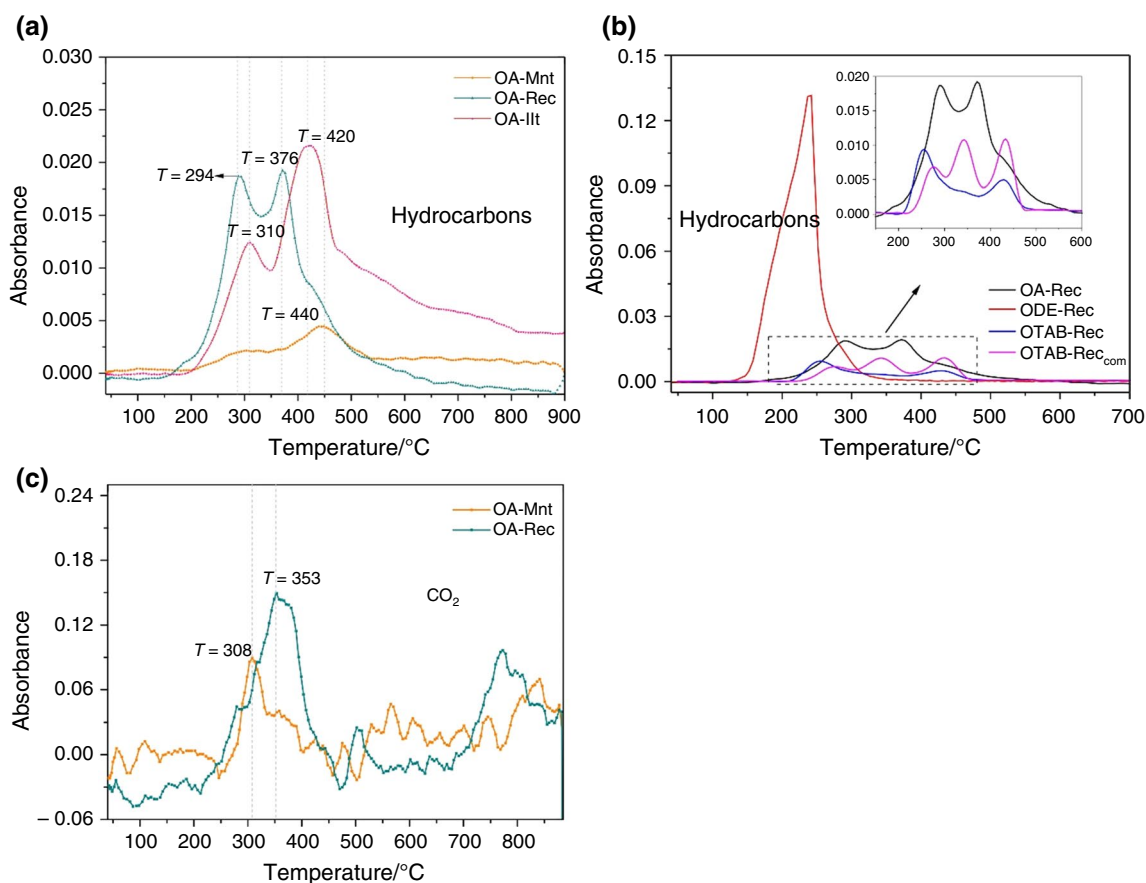


Fig. 5 FTIR absorbance vs. temperature curves of evolved hydrocarbons and CO₂ from pyrolyzed OM-clay complexes. **a** the curves of hydrocarbons for OA-Rec, OA-Mnt, and OA-Ilt; **b** the curves of

hydrocarbons for OA-Rec, OTAB-Rec, OTAB-Rec_{com}, and ODE-Rec; **c** the curves of CO₂ for OA-Rec and OA-Mnt

the temperature for generation of hydrocarbons [5, 11, 17]. As shown by the acidity determination, the Q_B in Rec (0.10 mmol/g) at room temperature was higher than that in Mnt (0.09 mmol/g). In particular, the Q_B in Rec was more than four times that of Mnt (Rec: 0.29 mmol/g; Mnt: 0.07 mmol/g) at the high temperature (350 °C) (Figure S4 in part III of SM).

Decarboxylation was reported to depend on L acid sites [22, 26], which mainly results from octahedral-coordinated Al³⁺ and/or Fe³⁺ ions exposed at the edges [42]. CO₂ was produced during the pyrolysis of OA-Rec while not in OA alone, suggesting that decarboxylation was prevalent in pyrolyzed OA-Rec but not in pyrolyzed pure OA (Table 2). Nevertheless, the Q_L in Rec (0.51 mmol/g) was much higher than that in Mnt (0.07 mmol/g) (Figure S4). According to a previous study, the decarboxylation of stearic acid occurred more readily with the minerals when the more basic Mg and Li populate the octahedral sheets of the clays than by Al and Fe ions [43]. In this study, Mnt contained some Mg–Al substitution structures compared with Rec according to FTIR analysis (Figure S3). Therefore, it can be inferred that the

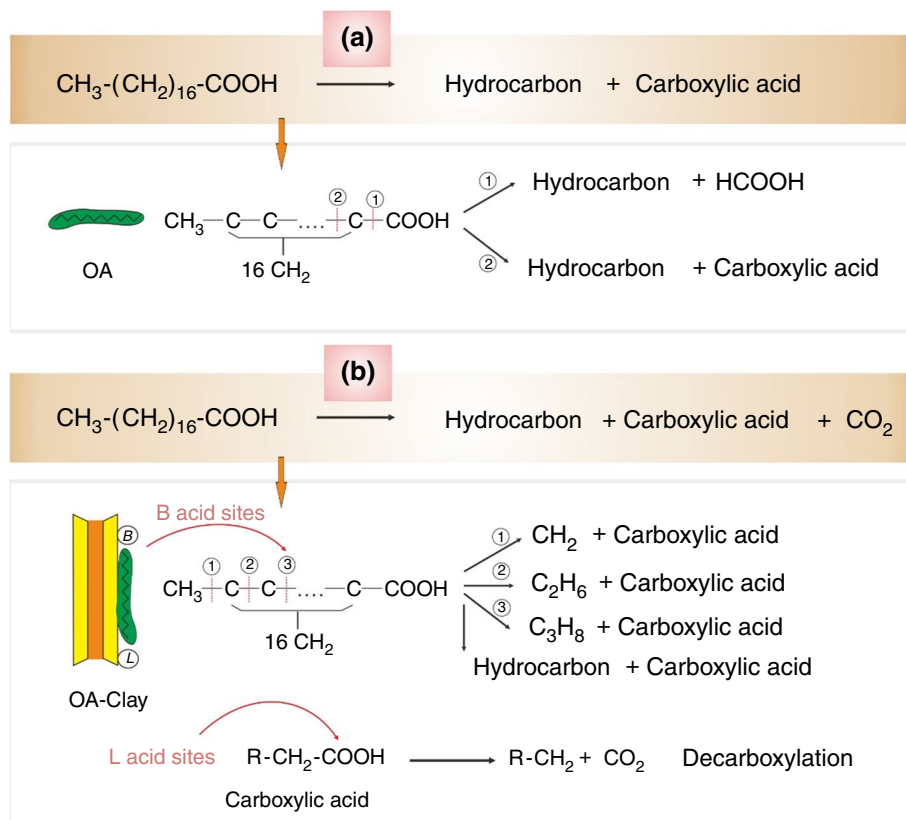
octahedral sheets of Mnt were more basic than that of Rec. Thus, an acid–base reaction on Mg-containing surfaces led to increased decarboxylation in the presence of Mnt. The above results seem to conclude that the degree of decarboxylation of fatty acid in OM-clay complexes still depended on the chemical composition of the octahedral sheets.

Interestingly, the presence of methyl gaseous hydrocarbons (a band at ~2966 cm⁻¹) further manifested the effect of I-Sm clay mineralogy in the pyrolysis process of OA. There was a significant peak for methyl gaseous hydrocarbon in the case of OA-Rec, but it almost did not occur in OA and OA-Ilt (Fig. 3). It appeared that C–C bond rupture mainly occurred between alkyl C and carboxyl C for pyrolysis of OA alone or in OA-Ilt, which led to the formation of carboxylic acid and the generation of long-carbon hydrocarbons (Fig. 6a). In contrast, for pyrolysis of OA in OA-Mnt and OA-Rec, the C–C bond cleavage reaction was promoted through carbonium ion pathways by the catalysis of B acid sites, producing methyl gaseous hydrocarbons (such as CH₄, C₂H₆, and C₃H₈). This result suggested that C–C bonds tend to break between alkyl C and alkyl C and away from

Table 2 The T_M , the main pyrolysis products, and pyrolysis mechanism of OMs/OM-Rec complexes

Types of OM	Functional groups	OMs/OM-clay complex	$T_M/^\circ\text{C}$	Gases product	Pyrolysis mechanism
Fatty acid	-COOH, -CH ₂ -CH ₃	OA	305	Hydrocarbons, carboxylic acid	C–C cleavage
		OA-Rec	276	Hydrocarbons, CO ₂ , carboxylic acid	carbonium ion pathway, decarboxylation
		OTAB	272	Hydrocarbons	S _N 2 nucleophilic substitution
Quaternary ammonium salt	-(CH ₃) ₃ N ⁺ , -CH ₂ -CH ₃	OTAB-Rec	241	Hydrocarbons, alkene	S _N 2 nucleophilic substitution, Hoffmann elimination
		OTAB-Rec _{com}	269, 343, 428	Hydrocarbons, alkene	S _N 2 nucleophilic substitution, Hoffmann elimination
Alkane	-CH ₂ -CH ₃	ODE	164, 247	Hydrocarbons	C–C cleavage
		ODE-Rec	233	Hydrocarbons	Carbonium ion pathway

Fig. 6 Schematic representation of the possible processes of pyrolysis of OA and OA-clay mixture: **a** C–C bond cleavage reaction of pyrolyzed OA alone; **b** C–C bond cleavage reaction and decarboxylation of OA-clay mixture. **b** does not include a description of Ill. The numerical symbols in the figure represent the locations of possible chemical bond breaks.



carboxyl C during the pyrolysis of OA in OA-Rec (Fig. 6b). These results suggested that the effect of Rec and Mnt were beneficial for breaking the C–C bonds of fatty acids away from carboxyl C. This behavior was closely related to abundant B acid sites catalysis of I-Sm clay minerals.

Effect of OM characteristics on the thermal evolution of OM-clay complexes

The above data indicated that the thermal evolution of the OM-clay complexes was closely related to the types of OMs.

Table 2 showed the T_M , main pyrolysis products, and pyrolysis mechanism of OM/OM-Rec complexes. Three types of OMs (including OA, OTAB, and ODE) and one kind of clay mineral Rec were discussed. Rec had contrasting effect on the pyrolysis of these OMs. For all OMs located into the external surface of Rec, the T_M of OMs was decreased by Rec. This result possibly depended on the catalytic activities of solid acid sites in clay minerals [44, 45]. B acid sites in Rec offer protons to trigger off the formation of carbocations [46, 47], which promoted the C–C bond breaking reaction, and it thus reduced the thermal temperature of the pyrolysis

reaction [48]. The H_3O^+ ions electrostatically captured by the negatively charged basal surface were the possible B acid sites [49, 50], and also the silanol (Si–OH) and aluminol (Al–OH₂OH) groups of clay minerals. Therefore, C–C cleavage by a carbocation mechanism was the pyrolysis reaction mechanism of OM-clay complexes, while C–C cleavage by a free radical mechanism was the pyrolysis reaction mechanism of OMs alone [5]. Probably for this reason, more hydrocarbons are present in the case of ODE-Rec. In addition to this, B acid sites could change the pyrolysis pathway of quaternary ammonium salt. For OTAB alone, the decomposition occurred following a $\text{S}_{\text{N}}2$ nucleophilic substitution reaction. While for OTAB-Rec complexes, the pyrolysis of OTAB can be promoted by the B acid sites through a Hoffmann elimination [8, 17], which lead to some alkene production.

To further investigate the effect of OM characteristics on the pyrolysis of OM-clay complexes, the characteristic band of hydrocarbons ($\sim 2934 \text{ cm}^{-1}$) for OM-Rec complexes corresponded pyrolysis of carbon chain were tracked with respect to temperature (Fig. 5b). The temperatures at which the hydrocarbons released followed the order: ODE-Rec < OA-Rec < OTAB-Rec < OTAB-Rec_{com}. The trend in the maximum hydrocarbon release temperature was ODE-Rec < OTAB-Rec < OA-Rec < OTAB-Rec_{com}. Previous studies have found that the bond energy of C–C and C–H was higher than that of C–O and C=O [51, 52]. It thus followed that the pyrolysis of OMs in this work was generally affected by Rec, owing to the binding effects between functional groups of OMs and Rec. For OA, the –COOH group was able to interact with hydroxyl ion in Rec through ligand exchange, cation bridging, and water bridging to some extent [53]. In this case, the interaction between OA and Rec needed additional energy to overcome compared with ODE and Rec. While for OTAB, the positive charge groups ($(\text{CH}_3)_3\text{N}^+$) in OM was easily adhered to the negative charge surface site of Rec because of the electrostatic interaction [54], and it even intercalated into interlayer space of Rec through cation exchange [55]. It thus caused a higher T_{M} and the difficulty of decomposition. It is because the electrostatic interaction and barriers effect of clay mineral sheet needed the additional energy to overcome [48]. For organic compound OTAB, however, the presence of a haloid anion (i.e., Br[–]) could decrease the thermal stability of quaternary alkyl ammonium-clay complexes [56, 57]. Therefore, compared with OA-Rec, the thermal evolution of OTAB-Rec was influenced, and the maximum hydrocarbon release temperature was lower than that of OA-Rec.

Conclusions

The results of our study showed that clay mineralogy had significant effects on the pyrolysis of OMs, which could lead to a decrease in the T_{M} and a change in the thermal pathways of pyrolysis OM. I-Sm clay minerals exhibited different effects on the peak temperature of hydrocarbon and CO_2 production. The thermal degradation of OA by effect of Rec was more pronounced than that by Mnt and Ilt. Rec-OA had lowest T_{M} and Ilt-OA had a similar thermal behavior with that of neat OA. These results were owing to the solid acidity of these clay minerals. B acid sites could promote the C–C bond cleavage reaction. L acid sites were responsible for the decarboxylation of OMs. Clay minerals (Mnt and Rec) with B acidity may influence the locations of C–C bond breaks, which leading to C–C bonds tend to break away from carboxyl C during the pyrolysis of OA. In addition to the solid acidity, the functional groups of OMs affected the interaction between clay and OMs, which thus leading to a different thermal evolution behavior (i.e., gaseous products). The interlayer structures for I-Sm clay minerals appeared to act as a barrier effect on the pyrolysis of OMs with the positive charge groups (i.e., OTAB). The findings demonstrated that the thermal evolution of aliphatic OMs was affected by the types of I-Sm clay minerals and the chemical structure of organic compound. The combined influence of surface reactive sites (i.e., solid acidity) and microstructure controlled the ability of I-Sm clay minerals to thermal evolution of OM. Further experiments involving natural OMs (i.e., kerogen), other clay minerals (i.e., mixed-layer kaolinite-smectite (K-Sm) minerals), and water are required to unravel the role of OM-clay interactions in hydrocarbon generation in the future work.

Supplementary Information The online version contains supplementary material available at <https://doi.org/10.1007/s10973-022-11829-z>.

Acknowledgements This work was financially supported by the National Natural Science Foundation of China (41802039; 41972046; 42025705; 42002040), GDAS' Project of Science and Technology Development (2020GDASYL-20200102019) and the Science and Technology Planning Project of Guangdong Province, China (2017BT01Z176).

Declarations

Conflict of interest The authors declare that they have no known competing financial interests or personal relationships that could have appeared to influence the work reported in this paper.

References

1. Newman SP, Di Cristina T, Coveney PV, Jones W. Molecular dynamics simulation of cationic and anionic clays containing amino acids. *Langmuir*. 2002;18(7):2933–9.

2. Ju Y, Wang G, Bu H, Li Q, Yan Z. China organic-rich shale geologic features and special shale gas production issues. *J Rock Mech Geotech Eng.* 2014;6(3):196–207.
3. Zhu X, Cai J, Liu W, Lu X. Occurrence of stable and mobile organic matter in the clay-sized fraction of shale: Significance for petroleum geology and carbon cycle. *Int J Coal Geol.* 2016;160:1–10.
4. Heller-Kallai L, Aizenshtat Z, Miloslavski I. The effect of various clay minerals on the thermal decomposition of stearic acid under “bulk flow” conditions. *Clay Miner.* 1984;19:779–88.
5. Yuan P, Liu H, Liu D, Tan D, Yan W, He H. Role of the interlayer space of montmorillonite in hydrocarbon generation: an experimental study based on high temperature–pressure pyrolysis. *Appl Clay Sci.* 2013;75:82–91.
6. Hower J, Eslinger EV, Hower ME, Perry EA. Mechanism of burial metamorphism of argillaceous sediment: I mineralogical and chemical evidence. *Geol Soc Am Bull.* 1976;87(5):725–37.
7. Abid I, Hesse R. Illitizing fluids as precursors of hydrocarbon migration along transfer and boundary faults of the Jeanne d’Arc Basin offshore Newfoundland. *Canada Mar Petrol Geol.* 2007;24:237–45.
8. Li Y, Cai J, Song G, Ji J. DRIFT spectroscopic study of diagenetic organic–clay interactions in argillaceous source rocks. *Spectrochim Acta A.* 2015;148:138–45.
9. Burst JF. Diagenesis of Gulf Coast clayey sediments and its possible relation to petroleum migration. *AAPG Bull.* 1969;53(1):73–93.
10. Pollastro RM. Considerations and applications of the illite/smectite geothermometer in hydrocarbon-bearing rocks of Miocene to Mississippian age. *Clays Clay Miner.* 1993;41(2):119–33.
11. Liu H, Yuan P, Qin Z, Liu D, Tan D, Zhu J, He H. Thermal degradation of organic matter in the interlayer clay–organic complex: a TG-FTIR study on a montmorillonite/12-aminolauric acid system. *Appl Clay Sci.* 2013;80–81:398–406.
12. Whitelaw P, Uguna CN, Stevens LA, Meredith W, Snape CE, Vane CH, Moss-Hayes V, Carr AD. Shale gas reserve evaluation by laboratory pyrolysis and gas holding capacity consistent with field data. *Nat Commun.* 2019;10(1):1–10.
13. Mackenzie AS, Li RW, Maxwell JR, Moldowan JM, Seifert WK. Molecular measurements of thermal maturation of Cretaceous shales from the Overthrust Belt, Wyoming, USA. *Advances in Org. Geochem.* 1981; Wiley Chichester, pp. 496–503.
14. Tannenbaum E, Huizinga BJ, Kaplan IR. Role of minerals in thermal alteration of organic matter–II: a material balance. *AAPG Bull.* 1986;70(9):1156–65.
15. Lewan MD. Experiments on the role of water in petroleum formation. *Geochim Cosmochim Acta.* 1997;61:3691–723.
16. Seewald JS. Aqueous geochemistry of low molecular weight hydrocarbons at elevated temperatures and pressures: constraints from mineral buffered laboratory experiments. *Geochim Cosmochim Acta.* 2001;65(10):1641–64.
17. Bu H, Yuan P, Liu H, Liu D, Liu J, He H, Zhou J, Song H, Li Z. Effects of complexation between organic matter (OM) and clay mineral on OM pyrolysis. *Geochim Cosmochim Acta.* 2017;212:1–15.
18. Song H, Liu H, Bu H, Liu D, Li Y, Du P. Effects of montmorillonite charge reduction on the high-temperature/high-pressure pyrolysis of organic matter. *Appl Clay Sci.* 2021;213: 106243.
19. Wu LM, Zhou CH, Keeling J, Tong DS, Yu WH. Towards an understanding of the role of clay minerals in crude oil formation, migration and accumulation. *Earth-Sci Rev.* 2012;115(4):373–86.
20. Hetényi M. Simulated thermal maturation of type I and III kerogens in the presence, and absence, of calcite and montmorillonite. *Org Geochem.* 1995;23(2):121–7.
21. Geatches DL, Clark SJ, Greenwell HC. Role of clay minerals in oil-forming reactions. *J Phys Chem A.* 2010;114(10):3569–75.
22. Johns WD, Shimoyama A. Clay minerals and petroleum-forming reactions during burial and diagenesis. *AAPG Bull.* 1972;56(11):2160–7.
23. Berthonneau J, Grauby O, Abuhaikal M, Pellenq RJM, Ulm FJ, Van Damme H. Evolution of organo-clay composites with respect to thermal maturity in type II organic-rich source rocks. *Geochim Cosmochim Acta.* 2016;195:68–83.
24. Guven N. On a definition of illite/smectite mixed-layer. *Clay Clay Miner.* 1991;39(6):661–2.
25. Bethke CM, Vergo N, Altaner SF. Pathways of smectite illitization. *Clays Clay Miner.* 1986;34:125–35.
26. Jurg JW, Eisma E. Petroleum hydrocarbons: generation from fatty acid. *Science.* 1964;144(3625):1451–2.
27. Liu W, Xu Y, Shi J, Lei H, Zhang B. Evolution model and formation mechanism of bio-thermocatalytic transitional zone gas. *SCI China Ser D.* 1997;40(1):43–53.
28. Wattel-Koekkoek EJW, Van Genuchten PPL, Buurman P, Van Lagen B. Amount and composition of clay-associated soil organic matter in a range of kaolinitic and smectitic soils. *Geoderma.* 2001;99(1–2):27–49.
29. Vranova V, Rejsek K, Formanek P. Aliphatic, cyclic, and aromatic organic acids, vitamins, and carbohydrates in soil: a review. *Sci World J.* 2013. <https://doi.org/10.1155/2013/524239>.
30. Rogers DE. Thermal analysis of octadecanoic acid and some of its salts. *Thermochim Acta.* 1984;77(1–3):123–32.
31. Shimoyama A, Johns WD. Catalytic conversion of fatty acids to petroleum-like paraffins and their maturation. *Nat Rev Phys.* 1971;232(33):140–4.
32. Zafar R, Watson JS. Adsorption of tetradecanoic acid on kaolinite minerals: using flash pyrolysis to characterise the catalytic efficiency of clay mineral adsorbed fatty acids. *Chem Geol.* 2017;471:111–8.
33. Daniels EJ, Altaner SP. Clay mineral authigenesis in coal and shale from the Anthracite region. *Pennsylvania Am Miner.* 1990;75:825–39.
34. Pozo M, Pino D, Bessieres D. Effect of thermal events on maturation and methane adsorption of Silurian black shales (Checa, Spain). *Appl Clay Sci.* 2017;136:208–18.
35. Hong H, Zhang X, Wan M, Hou Y, Du D. Morphological characteristics of (K, Na)-rectorite from Zhongxiang rectorite deposit, Hubei. *Central China J China Univ Geosci.* 2008;19(1):38–46.
36. Negrón-Mendoza A, Ramos S, Albarrán G. Enhance decarboxylation reaction of carboxylic acids in clay minerals. *Radiat Phys Chem.* 1995;46(4–6):565–8.
37. Liu D, Yuan P, Liu H, Cai J, Qin Z, Tan D, Zhou Q, He H, Zhu J. Influence of heating on the solid acidity of montmorillonite: a combined study by DRIFT and Hammett indicators. *Appl Clay Sci.* 2011;52(4):358–63.
38. Huang NP, Michel R, Voros J, Textor M, Hofer R, Rossi A, Spencer ND. Poly (L-lysine)-g-poly (ethylene glycol) layers on metal oxide surfaces: surface-analytical characterization and resistance to serum and fibrinogen adsorption. *Langmuir.* 2001;17(2):489–98.
39. Pitkänen I, Huttunen J, Halttunen H, Vesterinen R. Evolved gas analysis of some solid fuels by TG-FTIR. *J Therm Anal Calorim.* 1991;56(3):1253–9.
40. Jandura P, Kokta BV, Riedl B. Fibrous long-chain organic acid cellulose esters and their characterization by diffuse reflectance FTIR spectroscopy, solid-state CP/MAS ¹³C-NMR, and X-ray diffraction. *J Appl Polym Sci.* 2000;78(7):1354–65.
41. Marcilla A, Gómez A, Menargues S. TGA/FTIR study of the catalytic pyrolysis of ethylene–vinyl acetate copolymers in the presence of MCM-41. *Polym Degrad Stab.* 2005;89(1):145–52.
42. Rupert JP, Granquist WT, Pinnavaia TJ. Catalytic properties of clay minerals. In: Newman ACD, editor. *Chemistry of clays and*

- clay minerals. New York: Longman scientific and technical. 1987; 6: 275–318.
43. Goldstein TP. Geocatalytic reactions in formation and maturation of petroleum. *AAPG Bull.* 1983;67(1):152–9.
 44. Reddy CR, Bhat YS, Nagendrappa G, Prakash BJ. Brønsted and Lewis acidity of modified montmorillonite clay catalysts determined by FT-IR spectroscopy. *Catal Today.* 2009;141(1–2):157–60.
 45. Singh B, Patial J, Sharma P, Agarwal SG, Qazi GN, Maity S. Influence of acidity of montmorillonite and modified montmorillonite clay minerals for the conversion of longifolene to isolongifolene. *J Mol Catal A: Chem.* 2007;266(1–2):215–20.
 46. Johns WD. Clay mineral catalysis and petroleum generation. *Annu Rev Earth Planet Sci.* 1979;7(1):183–98.
 47. Greensfelder BS, Voge HH, Good GM. Catalytic and thermal cracking of pure hydrocarbons: mechanisms of Reaction. *Ind Eng Chem.* 1949;41(11):2573–84.
 48. Liu H, Yuan P, Liu D, Bu H, Song H, Qin Z, He H. Pyrolysis behaviors of organic matter (OM) with the same alkyl main chain but different functional groups in the presence of clay minerals. *Appl Clay Sci.* 2018;153:205–16.
 49. Newman ACD. Chemistry of clays and clay minerals. New York: Wiley-Inter science; 1987.
 50. Rupert JP, Granquist WT, Pinnavaia TJ. Catalytic properties of clay minerals. In: Newman ACD, editor. Chemistry of clays and clay minerals. New York: Longman scientific and technical. 1987; 6: 275–318.
 51. Shi L, Liu Q, Guo X, Wu W, Liu Z. Pyrolysis behavior and bonding information of coal—A TGA study. *Fuel Process Technol.* 2013;108:125–32.
 52. Mishra RK, Mohanty K. Thermal and catalytic pyrolysis of pine sawdust (*Pinus ponderosa*) and Gulmohar seed (*Delonix regia*) towards production of fuel and chemicals. *Mater Sci Tech Lond.* 2019;2(2):139–49.
 53. Underwood T, Erastova V, Cubillas P, Greenwell HC. Molecular dynamic simulations of montmorillonite–organic interactions under varying salinity: an insight into enhanced oil recovery. *J Phys Chem C.* 2015;119(13):7282–94.
 54. Xi Y, Ding Z, He H, Frost RL. Structure of organoclays—an X-ray diffraction and thermogravimetric analysis study. *J Colloid Interface Sci.* 2004;277(1):116–20.
 55. Ghavami M, Zhao Q, Javadi S, Jangam JSD, Jasinski JB, Saraei N. Change of organobentonite interlayer microstructure induced by sorption of aromatic and petroleum hydrocarbons—A combined study of laboratory characterization and molecular dynamics simulations. *Colloid Surfaces A.* 2017;520:324–34.
 56. Davis R, Gilman J, Sutto T, Callahan HJ, Trulove P, De Long H. Improved thermal stability of organically modified layered silicates. *Clay Clay Miner.* 2004;52(2):171–9.
 57. Cui L, Hunter DL, Yoon PJ, Paul DR. Effect of organoclay purity and degradation on nanocomposite performance, part 2: morphology and properties of nanocomposites. *Polymer.* 2008;49(17):3762–9.

Publisher's Note Springer Nature remains neutral with regard to jurisdictional claims in published maps and institutional affiliations.

Springer Nature or its licensor (e.g. a society or other partner) holds exclusive rights to this article under a publishing agreement with the author(s) or other rightsholder(s); author self-archiving of the accepted manuscript version of this article is solely governed by the terms of such publishing agreement and applicable law.